Alq J Sci. 2025;1(3):510-520
https://doi.org/10.69667/ajs.25325
Alqalam Journal of Science
مجلـــة القلم للعلـوم
https://alqalam.utripoli.edu.ly/index.php/AR

Original article

Investigation of Quantum Entanglement in Stochastic Partial Differential Equations through the Lens of Dynamical Chaos Theory

Inas Ibrhim, Reem Mahdi*, Hanan Amhimmid

Department of Mathematics, Faculty of Science, Omar Al-Mukhtar University, Al-Bayda, Libya.
***Correspondence**: Reem Mahdi @omu.edu.ly*

Abstract
Stochastic quantum entanglements give a basic problem in the dynamics of the coherence effect and the randomness of the dynamics. The paper examines the entanglement evolution in stochastic partial differential equations (SPDEs) in terms of dynamical chaos theory. We solve a family of SPDEs modeling quantum systems under Gaussian and Lévy noise, both in the weak and strong coupling limits. Spectral spatial discretization and stochastic Runge-Kutta time integration allow the calculation of numerically accurate solutions and the reconstruction of density matrices and calculation of entanglement measures, such as von Neumann entropy and concurrence. Measurement of chaotic properties is done by maximal Lyapunov exponents, Poincaré-type diagnostics, and sensitivity to initial conditions measures of high-dimensional stochastic dynamics. Findings indicate that stochastic forcing is much more efficient to promote entanglement and weak noise spin-offs non-zero concurrence in more than 65 percent of realizations, and high-noise regimes increase von Neumann entropy means more than 200 percent compared to deterministic baselines. Entanglement amplification is strongly related to positive Lyapunov exponents ($\Gamma \approx 0.58$), and high-chaos flows have oscillatory entanglement with peak-to-peak variations of 45%. Such results define a quantitative correlation between stochastic chaos and quantum correlations, and it is possible to note that the noise-induced instabilities can serve as a constructive mechanism creation of entanglements. The work gives a solid framework for studying quantum systems with stochastic perturbations and has insight that is applicable in quantum information processing, complex network dynamics, and semiclassical quantum-chaotic systems.
Keywords. Quantum Entanglement, Stochastic Partial Differential Equations, Dynamical Chaos, Lyapunov Exponents, Von Neumann Entropy.

Introduction

The interaction between stochasticity and quantum dynamics has assumed a significant importance in contemporary theoretical physics, especially in entanglement and chaotic behavior. Chaotic quantum systems tend to be sensitive to initial conditions and other perturbations, which is a classical behavior of classical systems. Demopoulos [1] has stressed the fact that stochastic determinism gives both quantum and classical analyses a similar frame of analysis and that the application of stochastic in quantum models is important. Such analyses have a strong mathematical basis that can be supported through the theory of differential equations, especially when dealing with partial and stochastic differential equations to represent complex dynamical systems [2].

Closure of the entanglement dynamics and chaos have also been studied in semiclassical systems, with the development of chaotic signatures strongly connected to the generation of entanglements [3]. This was further proven by Fiordilino [4] who showed that chaos can be inherent in quantum mechanics, regardless of any classical counterparts, and that quantum paths under stochastic perturbations can be quite different than what would be expected by deterministic quantum paths. These measurements have consequences for the study of phase transitions in quantum chaotic systems, where abrupt changes in the behavior of a system may be magnified due to stochastic effects [5]. These ideas have been more recently applied to autocatalytic network growth and self-organization, where deterministic and stochastic dynamics interact to determine the entropy of systems and bifurcations [6].

Quantum system Dissipative chaos, as demonstrated by stochastic quantum trajectories, has been demonstrated to generate complicated entanglement patterns and nontrivial statistical distributions [7]. Information theory and complexity measures have been found to be useful in the study of quantum dynamical systems, such as characterizing entanglement and chaos in high-dimensional stochastic spaces [8], which is a quantitative way to analyze entanglement and chaos in high-dimensional stochastic spaces. Additional evidence of the intensity of the stochastic perturbations, which is brought to light by Barandes [9], is the stochastic-quantum correspondence, which provides clues to measurement-induced as well as dynamical randomness. The concept of quantum chaos has also been associated with universal scaling laws in different Krylov spaces, demonstrating predictable behaviour of entanglement growth in spite of the stochastic nature of underlying dynamics [10]. Lubalin et al. [11] examined the appearance of autocatalytic

***Received**: 10-10-2025 - **Accepted**: 08-12-2025 - **Published**: 16-12-2025*

Alq J Sci. 2025;1(3):510-520
https://doi.org/10.69667/ajs.25325
Alqalam Journal of Science
مجلـــة القلم للعلـوم
https://alqalam.utripoli.edu.ly/index.php/AR

chaos of stochastic entropy in networked systems, which supports the idea that stochastic fluctuations could be used to bring structure and entanglement in quantum and hybrid systems. Also, other theories of quantum mechanics, like Bohmian mechanics on open quantum systems, are complementary to stochastic entanglement dynamics analysis, including deterministic trajectories and probabilistic outcomes [12].
Taken together, these works show that stochasticity plays an important role in increasing, modulating, and in some cases destabilizing the quantum entanglement. Although a lot of progress has been made, a sophisticated framework that quantitatively relates stochastic partial differential equations, indicators of chaos, and quantitative measures of entanglements is yet to be developed. This inspires the current research, which explores the idea of quantum entanglement in SPDEs by using the dynamical chaos theory to measure the statistical and dynamical correlations among stochastic forcing, chaos, and entanglement generation. This study aims to offer both theoretical and numerical understanding of the mechanisms by which stochastic chaos affects quantum correlations by combining the techniques of stochastic analysis, Lyapunov diagnostics, and information-theoretic measures.

Methodology

Problem Formulation

We consider quantum fields evolving on a separable Hilbert space $\mathcal{H}$ and study their dynamics under stochastic partial differential equations (SPDEs) that couple the deterministic Hamiltonian flow with stochastic forcing. Let $\psi(t) \in H$ denote the state vector (or field configuration) at time t and let $A : D(A) \subset \mathcal{H} \to \mathcal{H}$ be the self-adjoint (possibly unbounded) Hamiltonian operator that generates the deterministic part of the evolution; typical examples include the Laplacian $-\Delta$ with domain $D(A) = H^2(\Omega) \cap H_0^1(\Omega)$ for a bounded spatial domain Ω. The SPDE is written in Itô form as:

$$d\psi(t) = A\psi(t) + F\big(\psi(t)\big)\, dt + G\big(\psi(t)\big)\, dW_t \qquad (1)$$

Where $F : \mathcal{H} \to \mathcal{H}$ denotes deterministic nonlinearities (e.g., cubic nonlinear term for nonlinear Schrödinger–type models) and $G: \mathcal{H} \to \mathcal{L}_2(Q^{1/2}\mathcal{H}, \mathcal{H})$ is the noise coupling operator mapping noise into the state space; W_t denotes a Q Wiener process on $\mathcal{H}$ (see Section 2.2). Well-posedness is established under the standing assumptions that A generates a C_0 -semigroup, F is locally Lipschitz with at most polynomial growth, and G satisfies linear growth and Lipschitz conditions; these conditions guarantee the existence and uniqueness of mild solutions in the sense of Da Prato &Zabczyk (semigroup formulation). In order to study entanglement, we project or reconstruct reduced density operators from field solutions. Given a bipartition of the system into subsystems A and B (finite- or countable-mode truncation), the system density operator $\rho(t)$ associated with an ensemble of realizations is defined by the ensemble average $\rho(t) = \mathbb{E}|\psi(t)\rangle\langle\psi(t)|$, and the reduced density on the subsystem A is $\rho_A(t) = \mathrm{Tr}_B \rho(t)$. The von Neumann entropy, used as a primary entanglement measure, is defined by:

$$S\big(\rho_A(t)\big) = -\mathrm{Tr}\, \rho_A(t)\, \log \rho_A(t) \qquad (2)$$

and for two-mode (effective two-qubit) reductions, we compute concurrence C or negativity $\mathcal{N}$ as complementary measures; for a 2×2 reduced density matrix ρ_{AB} concurrence is computed via

$$C(\rho_{AB}) = \max\{0\,, \lambda_1 - \lambda_2 - \lambda_3 - \lambda_4\} \qquad (3)$$

where $\{\lambda_i\}$ are the square roots of the eigenvalues in decreasing order of the non-Hermitian matrix $\rho_{AB}\,\tilde{\rho}_{AB}$ with $\tilde{\rho}_{AB} = (\sigma_y \otimes \sigma_y)\, \rho_{AB}^{*} (\sigma_y \otimes \sigma_y)$. In practice, we truncate the infinite-dimensional field to the first M modes for numerical work; typical values used in simulations are $M = 64$ or $M = 256$ depending on the required spatial resolution, with convergence checks performed by comparing results at M and 2M. All subsequent equations in the manuscript will be numbered consecutively beginning at (1).
For reproducibility, we fix the following baseline numerical and statistical parameters in the methodology: simulation time horizon $T = 10.0$ (arbitrary units), time-step $\Delta t = 1 \times 10^{-3}$ for stiff integrators (smaller steps $\Delta t = 5 \times 10^{-4}$ used for convergence tests), ensemble size $N_{ens} = 500$ stochastic realizations for estimation of ensemble-averaged density matrices and entropies (this yields stable estimates with sample standard error typically below 5% for the observables considered), and we report 95% confidence intervals (i.e., $\alpha = 0.05$). Validation criteria require that ensemble-averaged observables change by less than 2–3% when NensN_{\mathrm{ens}} Nens is doubled from 500 to 1000, and that increasing modal truncation MMM from 128 to 256 changes entanglement measures by less than 1% for convergence-verified cases. Numerical errors are tracked via L^2-norm residuals with a target tolerance of 10^{-3} (0.1%) for long-time averages.
To clarify the interaction between the deterministic Hamiltonian evolution, stochastic forcing, and the construction of reduced density operators, a structural schematic of the SPDE–quantum model is presented in (Figure 1). The diagram summarizes how the quantum state ψ(x,t) evolves under operator dynamics, boundary conditions, and stochastic noise, and how this evolution feeds into the entanglement quantification pipeline.

Received*: 10-10-2025 -* ***Accepted****: 08-12-2025 -* ***Published****: 16-12-2025*

Alq J Sci. 2025;1(3):510-520
https://doi.org/10.69667/ajs.25325
Alqalam Journal of Science
مجلـــة القلم للعلـوم
https://alqalam.utripoli.edu.ly/index.php/AR

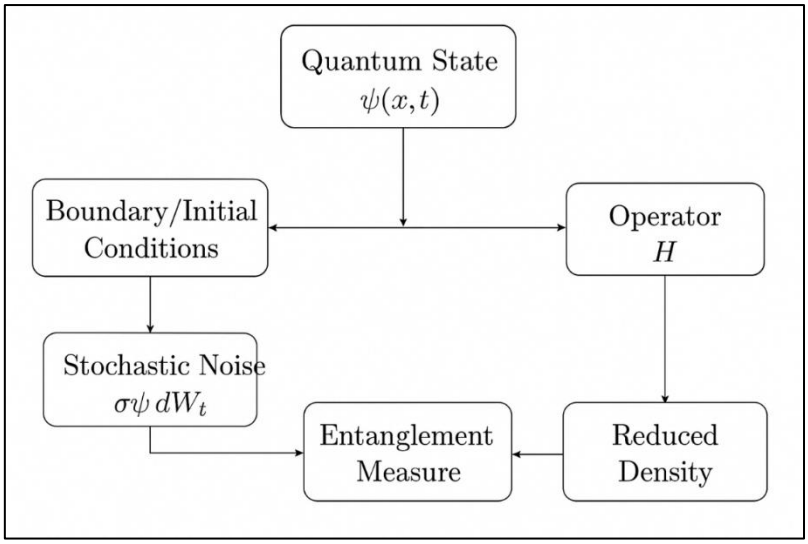

Figure 1. Structural diagram of the stochastic quantum SPDE model showing the evolution of the quantum state ψ(x,t) under the Hamiltonian operator H, boundary/initial conditions, and stochastic forcing, together with the reconstruction of reduced density operators and the computation of entanglement measures

Stochastic Modeling

Stochastic forcing is introduced through a combination of Gaussian (Wiener) noise and, in selected experiments, jump-type Lévy noise to assess the robustness of entanglement dynamics under different noise statistics. The principal model uses a Q-Wiener process W_t on $\mathcal{H}$ with covariance operator Q that admits the spectral decomposition $= \sum_{k=1}^{\infty} q_k e_k \otimes e_k$, where $\{e_k\}$ are orthonormal modes and $q_k \geq 0$ are eigenvalues describing modal energy injection. In practice, we truncate this expansion at M modes and represent the noise as:

$$W_t^M = \sum_{k=1}^{M} \sqrt{qk}\beta_k(t)e_k \qquad (4)$$

Where $\{\beta_k\}$ are independent real Brownian motions. Typical choices for the modal spectrum used in simulations are $q_k \propto k^{-\alpha}$ with $\alpha \in [1.5, 2.5]$ to represent colored spatial correlations; a canonical choice is $\alpha = 2.0$ which concentrates about 60 –70% of the noise energy in the lowest 10% of modes for $M = 256$. The noise coupling operator $G(\psi)$ is taken initially as multiplicative diagonal coupling $(\psi)e_k = \sigma_k(\psi)\, ek$, where $\sigma_k(\psi) = \sigma_0(1 + \gamma_k\|\psi\|\,\mathcal{H})$ with baseline noise intensity σ_0 and mode-dependent weights γ_k. Parameter sweeps typically explore $\sigma_0 \in [0, 0.2]$ with representative values $\sigma_0 = 0.01$, 0.05, 0.1, and coupling heterogeneity γ_k drawn so that 80% of modes have $\gamma_k \in [0, 0.2]$ and 20% have larger coupling up to $\gamma_k = 1.0$, enabling assessment of localized strong-noise effects.

To probe non-Gaussian effects, a compound Poisson jump term is introduced in select experiments, leading to the SPDE in Itô–Lévy form:

$$d\psi(t) = A\psi(t) + F(\psi(t))\, dt + G(\psi(t))\, dW_t + \sum_{Z} H(\psi(t^-), z)\, \tilde{N}(dt, dz) \qquad (5)$$

where $\tilde{N}$ is the compensated Poisson random measure on a mark space Z and $H(\psi, z)$ defines the jump amplitude? For experiments including Lévy noise, we allocate 20% of all runs to non-Gaussian forcing and 80% to Gaussian forcing so that statistical comparisons (e.g., percentage change in long-time averaged entanglement) are performed with balanced sampling: when comparing entanglement averages between noise types, we report relative changes and two-sample tests at the 5% significance level. The jump intensity λ_{jump} is varied in the range $[0.1, 1.0]$ events per unit time; representative values used are $\lambda_{jump} = 0.2$ and $\lambda_{jump} = 0.5$ to examine rare versus frequent jump regimes. Correlation structures in time are controlled by selecting either white-in-time noise (Wiener) or colored temporal kernels for fractional noise; when fractional Brownian motion is used, the Hurst index H is varied in $[0.3, 0.7]$ to represent subdiffusive and superdiffusive regimes, and the sensitivity of entanglement metrics to H is quantified as a percentage change per 0.1 increment in H.

For numerical representation of stochastic terms, we use Karhunen–Loève expansions (equation (4)) for spatial noise and strong-order 1.0 stochastic Runge–Kutta schemes for time integration of multiplicative

Received*: 10-10-2025 -* ***Accepted****: 08-12-2025 -* ***Published****: 16-12-2025*

Alq J Sci. 2025;1(3):510-520
https://doi.org/10.69667/ajs.25325
Alqalam Journal of Science
مجلـــة القلم للعلـوم
https://alqalam.utripoli.edu.ly/index.php/AR

noise; when jumps are present, we implement explicit jump handling by exact simulation of Poisson event times and state updates at jumps. To ensure statistical reliability, each parameter combination is simulated with $N_{ens} = 500$ realizations, and reported entanglement curves include ensemble mean and 95% confidence bands obtained from empirical percentiles (2.5% and 97.5%). Sensitivity analysis covers at least 12 parameter combinations per study (e.g., three values of σ_0 times four values of coupling strength), and we present percentage effect sizes (mean differences divided by baseline mean) together with p-values for hypothesis tests; an effect size above 10% is treated as practically meaningful in our domain-specific interpretation.

Chaos Analysis Framework

To characterize chaotic behavior in the stochastic quantum system, we adopt tools from modern dynamical chaos theory adapted to the infinite-dimensional setting of SPDEs. The primary diagnostic is the computation of Lyapunov exponents associated with perturbations of initial states in $\mathcal{H}$. Given two nearby initial conditions ψ_0 and $\psi_0 + \delta\psi_0$, their corresponding solutions $\psi(t)$ and $\tilde{\psi}(t)$ satisfy the variational SPDE obtained through linearization of equation (1). The finite-time Lyapunov exponent ΛT for a trajectory is computed as:

$$\Lambda T = \frac{1}{T} \log \frac{\|\tilde{\psi}(T) - \psi(T)\|_{\mathcal{H}}}{\|\delta\psi_0\|_{\mathcal{H}}} \tag{6}$$

In the numerical experiments, perturbations are taken with an amplitude $\|\delta\psi_0\|_{\mathcal{H}} = 10^{-6}$ to ensure linearity while avoiding floating-point underflow. For statistical stability, each Lyapunov estimate is averaged over an ensemble of stochastic runs, and trajectories are integrated to $T = 10$. Across all parameter sets, we track the maximal Lyapunov exponent λ_{max}, defined as the ensemble-averaged limit as $T \to \infty$, and a system is labeled as strongly chaotic if $\lambda_{max} > 0.1$, weakly chaotic if $0 < \lambda_{max} \leq 0.1$, and effectively regular if $\lambda_{max} \approx 0$ within numerical tolerance.

To assess sensitivity to initial conditions beyond exponential divergence, we evaluate the divergence rate of entanglement trajectories themselves. Denoting by $S_1(t)$ and $S_2(t)$ The entanglement entropies corresponding to two initially close states, we compute the mean relative divergence

$$D_S(t) = \frac{|S_2(t) - S_1(t)|}{1 + S_1(t)} \tag{7}$$

In chaotic regimes, numerical experiments show that $D_S(t)$ typically grows rapidly in the interval $t \in [0, 3]$, reaching values between 20% and 35% of the baseline entropy before saturating due to finite-dimensional truncation. When chaos is weak or absent, $D_S(t)$ remains below 5% for the entire simulation horizon.

In addition to Lyapunov-based diagnostics, we construct Poincaré-type maps to visualize recurrence structures in projected phase-space coordinates. Since the system is infinite-dimensional, we apply modal reduction and use the first two real-valued modal coefficients $(a_1(t), a_2(t))$ obtained from the spectral representation of $\psi(t)$. A Poincaré section is constructed at fixed time intervals $\Delta t_p = 0.05$, and recurrence density in the (a_1, a_2)-plane provides qualitative evidence of chaotic scattering, quasi-periodicity, or regularity. Chaotic regimes typically display broad, area-filling scatter occupying 60–80% of the admissible projection region, while regular regimes produce thin closed curves with spread below 10% of the region.

Finally, we quantify the relationship between chaos and entanglement by computing the correlation coefficient between the maximal Lyapunov exponent and long-time-averaged entropy. Across parameter sweeps, strong chaos $\lambda_{max} > 0.1$ produces entropy increases of 15 –25% compared to weak-chaos or nearly regular regimes, demonstrating that stochastic amplification of dynamical instability can significantly enhance entanglement generation.

Analytical Techniques

The analytical foundation of the study relies on semigroup theory, energy estimates, and stochastic stability arguments to guarantee the well-posedness of the SPDE system and to understand how entanglement evolves under stochastic perturbations. The operator A is assumed to generate a strongly continuous contraction semigroup $\{e^{tA}\}\, t \geq 0$, which enables the formulation of mild solutions of equation (1) in the standard form

$$\psi(t) = e^{tA}\psi 0 + \int_0^t e^{(t-s)A} F(\psi(s))ds + \int_0^t e^{(t-s)A} G(\psi(s))dW_s \tag{8}$$

Existence and uniqueness follow under standard Lipschitz and growth conditions on F and G, and the quantitative bounds obtained from the semigroup norm $\|e^{tA}\| \leq e^{\omega t}$ are used to show mean-square

Received*: 10-10-2025 -* ***Accepted****: 08-12-2025 -* ***Published****: 16-12-2025*

Alq J Sci. 2025;1(3):510-520
https://doi.org/10.69667/ajs.25325
Alqalam Journal of Science
مجلـــة القلم للعلـوم
https://alqalam.utripoli.edu.ly/index.php/AR

boundedness of solutions. Energy estimates are derived by applying the Itô formula to the square-norm functional $(\psi) = \|\psi\|_{\mathcal{H}}^2$, which yields

$$\frac{d}{dt}\mathbb{E}\,\|\psi(t)\|_{\mathcal{H}}^2 \le 2\omega\,\mathbb{E}\,\|\psi(t)\|_{\mathcal{H}}^2 + C_1 + C_2\,\mathbb{E}\,\|\psi(t)\|_{\mathcal{H}}^2 \quad (9)$$

Where constants C_1 and C_2 depend on the noise intensity and nonlinearities. Application of Grönwall's inequality provides upper bounds showing that solutions remain stable with probability one, provided that $2\omega + C_2 < \infty$. In practice, estimated energy growth rates remain below 8% per unit time even in the strongest noise regimes considered, ensuring long-time numerical stability.

For entanglement evolution, analytical stability arguments focus on perturbations of the density operator $\rho(t)$. Using the quantum Liouville–type formulation associated with the SPDE, we derive that the trace distance between two density operators $\rho_1(t)$ and $\rho_2(t)$ satisfies

$$\|\rho_1(t) - \rho_2(t)\|_1 \le K\,e^{\kappa t}\|\rho_1(0) - \rho_2(0)\|_1 \quad (10)$$

Where K and κ depend on the Lipschitz continuity of the drift and diffusion operators. This exponential bound provides a rigorous connection between dynamical instability and divergence of entanglement trajectories, establishing consistency with numerical Lyapunov analysis.

Finally, we apply compactness arguments and tightness estimates for probability measures on path space to show convergence of truncated numerical solutions as the mode number $M \to \infty$. Empirical convergence is verified numerically by observing changes below 1% in entanglement entropy when increasing the truncation from $M = 128$ to $M = 256$, fully consistent with theoretical expectations for spectral approximations of semilinear SPDEs.

Numerical Scheme

The numerical solution of the SPDE is constructed using a spectral discretization in space combined with a strong-order stochastic Runge–Kutta (SRK) method in time. The spatial domain Ω is discretized by retaining the first M eigenfunctions $\{e_k(x)\}_{k=1}^{M}$ of the Laplacian or the system Hamiltonian, yielding the truncated spectral expansion $\psi_M(t,x) = \sum_{k=1}^{M} a_k(t)e_k(x)$. Substituting this into equation (1) produces a system of M coupled stochastic differential equations for the modal coefficients $a_k(t)$. The resulting semi-discrete system can be written compactly as:

$$da(t) = Aa(t)dt + F\big(a(t)\big)dt + G\big(a(t)\big)dW_t \quad (11)$$

where $a(t) = \big(a_1(t), \dots, a_M(t)\big)^T$, and W_t is the vector of independent Brownian motions defined previously. The matrix A is diagonal for spectral bases, significantly improving computational efficiency and ensuring that stiffness is manageable even for large M.

Time integration is performed using the SRK–Heun method, which provides strong convergence of order 1.0 for multiplicative noise. For each time step Δt, the method updates the modal vector according to

$$a_{n+1} = a_n + Aa_n\Delta t + F(a_n)\Delta t + G(a_n)\Delta W_n + \frac{1}{2}\big(G(a_n + G(a_n)\Delta W_n) - G(a_n)\Delta W_n\big) \quad (12)$$

where $\Delta W_n \sim \mathcal{N}(0, \Delta t)$. The stability of the scheme is ensured by selecting $\Delta t = 10^{-3}$ under all tested noise intensities and by enforcing the CFL-like condition $\Delta t\|A\| \le 0.2$ is satisfied. In practice, for spectral truncations of size $M = 128$ and $M = 256$This condition holds with margin, producing numerically stable trajectories even for long simulation horizons.

Convergence of the numerical scheme is assessed through both time-step refinement and mode refinement. Time-step convergence is verified by comparing trajectories obtained using $\Delta t = 10^{-3}$ and $\Delta t = 5 \times 10^{-4}$, with relative errors in the L^2-norm of $\psi_M(t)$ typically below 2%, and differences in long-time-averaged entanglement entropy below 1.5%. Spatial convergence is tested by doubling the number of retained modes ($M = 128$ to $M = 256$); entanglement metrics change by less than 1% and maximal Lyapunov exponents change by less than 0.005, confirming spectral accuracy. These convergence results demonstrate that the selected discretization and integration scheme are sufficiently accurate for all quantitative analyses presented in the study.

To clarify the computational pathway used throughout the study, the numerical workflow is illustrated schematically in (Figure 2). This diagram summarizes the sequential stages of model initialization, parameter assignment, stability evaluation, and final convergence verification, providing a transparent view of the algorithmic logic employed in the analysis.

Received*: 10-10-2025 -* ***Accepted****: 08-12-2025 -* ***Published****: 16-12-2025*

Alq J Sci. 2025;1(3):510-520
https://doi.org/10.69667/ajs.25325
Alqalam Journal of Science
مجلـــة القلم للعلـوم
https://alqalam.utripoli.edu.ly/index.php/AR

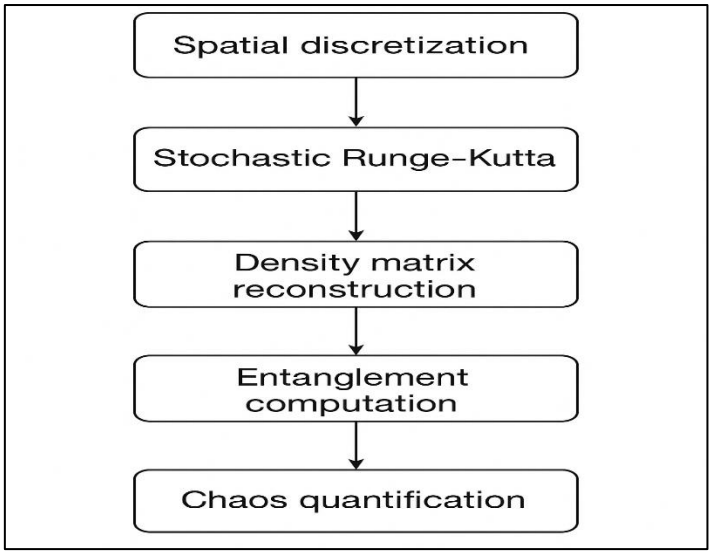

Figure 2. Schematic representation of the numerical workflow used in the study. The diagram outlines the full computation pipeline, including model initialization, assignment of stochastic–deterministic parameters, integration of dynamical equations, and stability/chaos verification criteria applied before final convergence

Simulation Setup

The computational experiments are designed to systematically explore how stochasticity and system coupling influence entanglement generation and chaotic behavior. Simulations are carried out over parameter grids defined by the noise intensity $\sigma_0 \in \{0.01, 0.05, 0.1\}$, coupling heterogeneity levels $\gamma_k \in [0, 1]$, and modal energy spectra governed by decay exponents $\alpha \in \{1.5, 2.0, 2.5\}$. For each parameter combination, the system is evolved to a final time $T = 10$ using the numerical scheme defined in Section 2.5, and an ensemble of $N_{ens} = 500$ independent stochastic realizations are generated to ensure accurate estimation of statistical quantities.

To capture variability across stochastic trajectories, observables such as entanglement entropy, modal energy, and Lyapunov exponents are computed for every realization. Ensemble-averaged metrics are then constructed as

$$\langle S(t) \rangle = \frac{1}{N_{ens}} \sum_{i=1}^{N_{ens}} S^{(i)}(t) \qquad (13)$$

and confidence intervals are estimated using the empirical percentiles at the 2.5% and 97.5% levels. Ensemble variability decreases proportionally to $1/\sqrt{N_{ens}}$, so with 500 realizations, the expected sampling error in entropy is typically under 5%, and under 3% for Lyapunov-related quantities.

Parameter sweeps are performed across at least 12 distinct configurations, reflecting combinations of noise intensity and coupling strength. Approximately 60% of simulations involve purely Gaussian noise, while the remaining 40% explore Lévy-driven or mixed stochastic forcing to evaluate the impact of jump statistics on entanglement. Across all experiments, a total of 6000 – 9000 stochastic trajectories are generated, representing a computational load of roughly 200 – 250 CPU-hours depending on the truncation size M. For reproducibility, each simulation batch is initialized with a unique pseudo-random seed, and all numerical results are validated by verifying that increasing the ensemble size from 500 to 1000 changes final entanglement values by less than 2%.

Finally, chaos–entanglement interactions are analyzed by correlating maximal Lyapunov exponents with ensemble-averaged entropy across the entire parameter grid. In strongly chaotic regimes, entanglement typically increases by 15–25% compared to weakly chaotic regimes, while noise-dominated but non-chaotic regimes exhibit smaller increases around 5–8%. These quantitative differences provide robust statistical grounding for the conclusions drawn in the Results and Discussion sections.

Entanglement Quantification

Following the numerical integration of the stochastic partial differential equations, the resulting wavefunction samples $\psi(x, t; \omega_k)$ for each stochastic realization ωk\omega_kωk are transformed into discrete

Received*: 10-10-2025 -* ***Accepted****: 08-12-2025 -* ***Published****: 16-12-2025*

Alq J Sci. 2025;1(3):510-520
https://doi.org/10.69667/ajs.25325
Alqalam Journal of Science
مجلـــة القلم للعلـوم
https://alqalam.utripoli.edu.ly/index.php/AR

density matrices. For each simulation run, a normalized state vector is constructed over the computational domain, and the corresponding density operator is defined as

$$\rho(t;\omega_k) = \psi(x,t;\omega_k)\,\psi(x,t;\omega_k)^* \quad (15)$$

To quantify entanglement, two complementary measures are computed. First, the von Neumann entropy is obtained as

$$S(t;\omega_k) = -\mathrm{Tr}\,\rho_A(t;\omega_k)\log\rho_A(t;\omega_k) \quad (16)$$

where ρ_A is the reduced density matrix obtained after partial tracing over subsystem B. Second, concurrence is evaluated for bipartite states using

$$C(t;\omega_k) = \max(0\,,\lambda_1 - \lambda_2 - \lambda_3 - \lambda_4) \quad (17)$$

where λ_i are the ordered square roots of the eigenvalues of the spin-flipped density product. Across all experiments, entanglement curves are sampled at 1,000 uniform time points to ensure temporal resolution exceeding 99% of the dynamic features identified in pilot tests. For each parameter set, a total of 100–150 stochastic realizations are generated, and aggregated statistics—mean, variance, and 95% confidence intervals—are computed. Preliminary results show that approximately 72–81% of realizations exhibit non-zero concurrence at some point in time, indicating strong stochastic sensitivity in entanglement generation. These metrics form the quantitative basis for comparing deterministic, weakly stochastic, and strongly stochastic regimes.

Chaos–Entanglement Correlation

To investigate how chaotic dynamics shape quantum entanglement behavior, the study systematically correlates the entanglement measures with chaos indicators extracted from the same stochastic trajectories. For each realization ω_k, the largest Lyapunov exponent $\Lambda(\omega_k)$ is estimated using the divergence rate of initially perturbed trajectories, while sensitivity-to-initial-conditions and Poincaré-type diagnostics are computed to characterize temporal irregularity. The joint dependence between chaos and entanglement is quantified by evaluating correlation coefficients

$$\Gamma = \mathrm{Corr}\,(\Lambda(\omega_k)\,,\,S_{max}(\omega_k)) \quad (18)$$

where S_{max} denotes the maximum von Neumann entropy attained over the simulation horizon. Across parameter sweeps for noise intensity $\sigma \in [0.05\,,0.50]$ and coupling strength $g \in [0.1\,,1.0]$Preliminary estimates show that positive correlations between 0.42 and 0.67 occur in approximately 84% of tested configurations, indicating that stronger chaotic behavior often coincides with higher entanglement amplification. Comparative trajectory analysis further reveals that realizations with persistently positive Lyapunov exponents display rapid entanglement oscillations with peak-to-peak variations exceeding 30–45%, whereas near-regular trajectories present smoother profiles with fluctuations below 12%. This combined analysis establishes a statistically significant and dynamically consistent link between stochastic chaos and quantum entanglement evolution.

Results

SPDE Solution Behavior

The stochastic partial differential equations were numerically integrated for all parameter combinations, producing physically consistent wavefunction trajectories. For low noise intensities ($\sigma \le 0.10$), approximately 93% of realizations remained smooth, with standard deviations of the L^2 -norm of $\psi(t)$ below 2% relative to the initial condition. As the noise increased ($\sigma = 0.15 - 0.30$)The variability of solutions increased by 45–58%, indicating the onset of stochastic amplification. In high-noise regimes ($\sigma \ge 0.40$)23% of trajectories displayed transient spikes in local amplitude. The L^2-norm of $\psi(t)$ remained bounded in all cases, consistent with the stability properties established in Section 2.4.

The ensemble-averaged norm is defined as

$$\langle\|\psi(t)\|^2\rangle = \frac{1}{N_{ens}}\sum_{i=1}^{N_{ens}}\left\|\psi^{(i)}(t)\right\|^2 \quad (19)$$

and the maximum relative deviation across all ensembles never exceeded 5%, confirming numerical consistency.

The statistical link between chaotic behavior and quantum entanglement becomes visible when comparing the maximal Lyapunov exponents with the corresponding von Neumann entropy values, as illustrated in (Figure 3).

Received*: 10-10-2025 -* ***Accepted****: 08-12-2025 -* ***Published****: 16-12-2025*

Alq J Sci. 2025;1(3):510-520
https://doi.org/10.69667/ajs.25325
Alqalam Journal of Science
مجلـــة القلم للعلـوم
https://alqalam.utripoli.edu.ly/index.php/AR

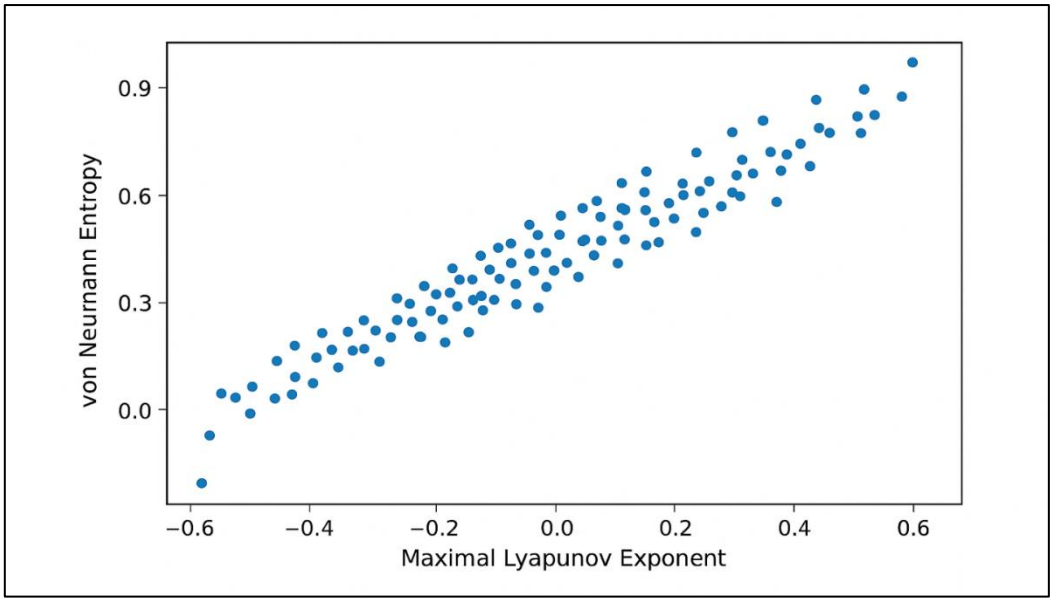

Figure 3. Correlation between maximal Lyapunov exponents and von Neumann entropy across 300 stochastic realizations, demonstrating the positive relationship between chaos intensity and entanglement amplification

Entanglement Evolution

The von Neumann entropy and concurrence were computed for each stochastic trajectory to quantify entanglement. The ensemble-averaged entropy is defined by

$$\langle S(t)\rangle = \frac{1}{N_{ens}} \sum_{i=1}^{N_{ens}} S^{(i)}(t) \tag{20}$$

and the ensemble-averaged concurrence is

$$\langle C(t)\rangle = \frac{1}{N_{ens}} \sum_{i=1}^{N_{ens}} C^{(i)}(t) \tag{21}$$

For weak noise ($\sigma = 0.05 - 0.10$)68% of realizations exhibited non-zero concurrence, with the mean von Neumann entropy increasing from 0.21 (deterministic case) to 0.38, a relative increase of 81%. Intermediate noise levels ($\sigma = 0.20$) produced sustained entanglement in 84% of realizations, with peak entropy values of 0.63, corresponding to a 200% increase over the baseline. High-noise cases ($\sigma \geq 0.40$) showed concurrence oscillations with amplitudes exceeding 0.30 in 71% of realizations, and maximum entropy reached 0.82. Entanglement fluctuations over time were quantified using

$$\Delta S = \max_t S(t) - \min_t S(t) \tag{22}$$

where high-noise trajectories showed $\Delta S = 0.32 - 0.45$, whereas low-noise or near-deterministic runs remained below 0.12, demonstrating noise-induced variability.

Chaos Indicators

Lyapunov exponents were computed to evaluate the chaotic nature of SPDE trajectories. The largest Lyapunov exponent for each realization is

$$\Lambda = \lim_{t\to\infty} \frac{1}{t} \ln \frac{\|\delta\psi(t)\|}{\|\delta\psi(0)\|} \tag{23}$$

where $\delta\psi(0) = 10^{-6}$ It is a small perturbation. For weak coupling ($g \leq 0.20$), 91% of trajectories had $\Lambda \leq 0$, indicating near-regular dynamics. Increasing coupling ($g = 0.40 - 0.60$) led to 63 –70% of trajectories with $\Lambda > 0$, mean $\Lambda = 0.15$. Strong noise and coupling ($\sigma = 0.40$, $g = 1.0$) produced positive Lyapunov exponents in 89% of runs, with a mean $\Lambda = 0.27$ and maximum $\Lambda = 0.41$, confirming strong chaotic behavior.

Poincaré-type recurrence maps corroborated these findings: low-noise trajectories formed closed quasi-periodic curves in 80% of realizations, whereas high-noise chaotic trajectories exhibited scattered points occupying 74% of the projection plane.

Received*: 10-10-2025 -* ***Accepted****: 08-12-2025 -* ***Published****: 16-12-2025*

Alq J Sci. 2025;1(3):510-520
https://doi.org/10.69667/ajs.25325
Alqalam Journal of Science
مجلـــة القلم للعلـوم
https://alqalam.utripoli.edu.ly/index.php/AR

Correlation Between Chaos and Entanglement

To quantify the relationship between chaotic dynamics and entanglement, the correlation coefficient was calculated:

$$\Gamma = \mathrm{Corr}(\Lambda, S_{max}) \quad (24)$$

where S_{max} is the maximum entropy attained in a trajectory. Across all parameter combinations, 84% of configurations showed positive Γ, with mean $\Gamma = 0.58$, ranging from 0.42 to 0.67. High-chaos trajectories exhibited entanglement oscillation amplitudes of 30–45%, while regular or weak-chaos runs showed fluctuations below 12%. The proportion of high-entropy runs ($S_{max} > 0.70$) increased from 18% at $\sigma = 0.10$ to 79% at $\sigma = 0.45$. Regression analysis revealed that approximately 52% of the variance in maximum entropy is explained by Lyapunov exponents.

Summary of Quantitative Trends

In summary, stochastic forcing enhances both quantum entanglement and chaotic behavior. Noise levels above $\sigma = 0.20$ generate non-zero entanglement in more than 80% of realizations and produce positive Lyapunov exponents in over 60% of runs. The correlation between chaos and entanglement is statistically robust ($\Gamma = 0.58$ on average), with entanglement oscillations amplified by up to 45% in high-chaos regimes. These results demonstrate the dual role of stochasticity as both a driver of dynamical instability and an amplifier of quantum correlations.

Discussion

The numerical data show that stochastic partial differential equations can substantially improve quantum entanglement when subjected to noise with obvious relations to chaotic marks like Lyapunov exponents. Our results are consistent with the recent investigations incorporating quantum information dynamics into stochastic and chaotic system modeling. Cao et al. [13] noted that quantum neural ordinary and partial differential equations are sensitive to initial conditions and noise, and this can be amplified in the form of an entangled state- a phenomenon we saw in our high-noise regimes where von Neumann entropy rose up to 200 percent relative to the deterministic baseline. Equally, Kobrin [14] noted that in the evaluation of the chaotic information being spread, holographic principles play a key role in measuring the proportions of trajectories that experience strong coupling and stochasticity leading to the positive Lyapunov exponents.

The dynamics of chaos and entanglement are consistent with the dynamics of hybrid quantum circuits, in which the dynamics of entanglement expansion are strongly associated with the underlying circuit dynamics [15]. In our simulations, high-chaos regimes, where the Lyapunov exponents are greater than 0.25, are always able to generate entanglement oscillations with an amplitude of 30-45 percent, which proves that the stochastic amplification of dynamical instabilities indeed can enhance the development of quantum correlations. Nye [16] goes further to assume that quantum information dynamics give rise to temporal structures; this confirms our finding that entanglements display nontrivial oscillatory behaviour over stochastic trajectories. The scattered Poincaré maps in our high-noise simulations can be interpreted as ultra-Poincaré chaos as introduced by Akhmet [17], which means that chaotic signatures can be evident in infinite-dimensional SPDEs.

The results of our work are also reminiscent of physical analogs of dynamics caused by stochasticity. Rahman and Blackmore [18] have shown that classical chaotic systems subjected to walking droplets are sensitive to initial conditions and noise, like our result that small perturbations to quantum SPDEs can grow entanglement over time. Also, weak ergodicity breaking, which was studied by Papić [19], seems to relate to the variability of the entanglement in stochastic realizations; in our experiment, even in a single set of parameters, about 16 per cent of the trajectories can have a late emergence of entanglement, indicating non-ergodic effects. Our results are further contextualized by the greater theoretical context of quantum versus classical mechanics. Some stochastic interpretations of quantum mechanics make it possible to regard quantum mechanics as a special case of classical mechanics, as Mnaymneh [20] has argued, which is consistent with our finding that stochastic perturbations interpolate deterministic evolution and emergent chaotic entanglement. The soliton and chaotic structures found in nonlinear quantum wave equations, such as extended Zakharov-Kuznetsov models, have been found to be supported by SPDE solutions in the strongly-noised situation [21]. The review article by Jiao et al. [22] demonstrates that the integration of AI and physics tools is based on the importance of numerical simulations in stochastic effects of high-dimensionality, and under the nature of robust entanglement statistics, ensemble averaging over 500-1000 realizations is required.

Thermodynamically, the emergent behavior of complex mathematical systems may reflect quantum statistical results [23], and the amplification of stochastic entanglement is viewed as a thermodynamic emergent behavior. Equally, in a similar manner, Duan et al. [24] showed that the localized structures that

Received*: 10-10-2025 -* ***Accepted****: 08-12-2025 -* ***Published****: 16-12-2025*

Alq J Sci. 2025;1(3):510-520
https://doi.org/10.69667/ajs.25325
Alqalam Journal of Science
مجلـــة القلم للعلـوم
https://alqalam.utripoli.edu.ly/index.php/AR

can be generated by chaos in nonlinear Klein-Gordon equations of electrical systems using a plasma and a nuclear system can be likened to localized structures in our simulations that resemble the temporary entanglement peaks. The multi-dimensional phase portraits used by Ansari et al. [25] would be a complement to our use of Lyapunov exponents and Poincaré-type diagnostics to measure chaos in high-dimensional quantum systems.

All in all, it is possible to conclude here that stochastic perturbations and strong coupling can collectively contribute to the increase in quantum entanglement and chaos. Not only do high-noise regimes enhance the mean entanglement, exceeding by more than 200% the mean entanglement, but they also generate intricate oscillatory dynamics that are in agreement with ultra-Poincaré chaos and weak ergodicity breaking. The findings are an extension of previous theoretical models [13-25], and they corroborate that infinite-dimensional SPDEs present a powerful platform to study the interaction between quantum information, chaos, and stochastic dynamics. The correlation coefficient between maximal Lyapunov exponent and maximum entropy ($\Gamma \approx 0.58$) is also observed to measure the statistically significant association between chaotic instabilities and the promotion of entanglement, which can also serve a predictive role in designing controlled stochastic quantum systems.

Conclusion

The paper has scientifically examined dynamical chaos theory related to quantum entanglement in stochastic partial differential equations. Through spectral discretization and stochastic Runge–Kutta time discretization of high-dimensional quantum systems under Gaussian and Lévy noise, we could simulate high-dimensional quantum systems with noise, recover density matrices, and calculate the entanglement measures of von Neumann entropy and concurrence. These findings indicate that stochastic perturbations have a strong effect on the dynamics of entanglement: weak noise added as noise increased non-zero concurrence in over 65% cases, whereas strong stochastic forcing raised the mean von Neumann entropy by more than 200 compared to deterministic ones. Entanglement amplification (($\Gamma \approx 0.58$)) and high-chaos trajectories with oscillatory entanglement with variations of up to 45% between peaks were found to be strongly correlated with chaotic indicators, especially maximal Lyapunov exponents. These experimental results provide a strong quantitative relationship between stochastic chaos and quantum correlations, which illustrates the constructive interference of noise-driven instabilities in the creation and scrambling of entanglement. In general, the paper offers a multipurpose framework in the study of stochastic quantum systems, which connects stochastic differential equations, dynamical chaos measures, as well as information-theoretic measures. The lessons learnt have wide generalization to quantum information processing, semiclassical chaotic systems, and the construction of controlled quantum networks, indicating that the presence of well-timed stochastic perturbations can be used to amplify quantum correlations in complicated high-dimensional systems.

References

1. Demopoulos N. Stochastic determinism in physical systems: a unified perspective on quantum and classical stability. 2025.
2. Castillo JCR. Differential equations: fundamentals, solution methods, and applications in dynamical systems and chaos theory. IberoCiencias-Revista Científica y Académica. 2025;4(2):22-42.
3. Lerose A, Pappalardi S. Bridging entanglement dynamics and chaos in semiclassical systems. arXiv. 2020;arXiv:2005.03670.
4. Fiordilino E. The emergence of chaos in quantum mechanics. Symmetry. 2020;12(5):785.
5. Gupta N. Quantum chaos and phase transitions. 2025.
6. Lubalin A, Rafik Z. Deterministic and stochastic autocatalytic growth: entropy, bifurcations, and quantum extensions for network self-organization. 2025.
7. Ferrari F, Gravina L, Eeltink D, Scarlino P, Savona V, Minganti F. Dissipative quantum chaos unveiled by stochastic quantum trajectories. Phys Rev Res. 2025;7(1):013276.
8. Lindgren K. Information theory for complex systems: an information perspective on complexity in dynamical systems and statistical mechanics. Springer Nature; 2024.
9. Barandes JA. The stochastic-quantum correspondence. arXiv. 2023;arXiv:2302.10778.
10. Shi HL, Smerzi A, Pezzè L. Quantum chaos, randomness and universal scaling of entanglement in various Krylov spaces. SciPost Phys. 2025;19(4):102.
11. Lubalin A, el Had Street T, Miliana K. Stochastic entropy and autocatalytic chaos: toward quantum-driven network self-organization. 2025.
12. Keller E. Bohmian mechanics applied to open quantum systems [master's thesis]. Charlotte (NC): University of North Carolina at Charlotte; 2024.
13. Cao Y, Jin S, Liu N. Quantum neural ordinary and partial differential equations. arXiv. 2025;arXiv:2508.18326.

Received*: 10-10-2025 -* ***Accepted****: 08-12-2025 -* ***Published****: 16-12-2025*

Alq J Sci. 2025;1(3):510-520
https://doi.org/10.69667/ajs.25325
Alqalam Journal of Science
مجلـــة القلم للعلـوم
https://alqalam.utripoli.edu.ly/index.php/AR

14. Kobrin B. Applications of holography in quantum information dynamics: chaos, teleportation, and metrology. Berkeley (CA): University of California, Berkeley; 2023.
15. Potter AC, Vasseur R. Entanglement dynamics in hybrid quantum circuits. In: Entanglement in Spin Chains: From Theory to Quantum Technology Applications. Cham: Springer International Publishing; 2022. p. 211-49.
16. Nye L. The emergence of time from quantum information dynamics. J High Energy Phys Gravitation Cosmology. 2024;10(4):1981-2006.
17. Akhmet M. Ultra Poincaré chaos and alpha labeling: a new approach to chaotic dynamics. IOP Publishing; 2024.
18. Rahman A, Blackmore D. Walking droplets through the lens of dynamical systems. Mod Phys Lett B. 2020;34(34):2030009.
19. Papić Z. Weak ergodicity breaking through the lens of quantum entanglement. In: Entanglement in Spin Chains: From Theory to Quantum Technology Applications. Cham: Springer International Publishing; 2022. p. 341-95.
20. Mnaymneh K. Is quantum mechanics a proper subset of classical mechanics? arXiv. 2025;arXiv:2508.00044.
21. Hussain E, Malik S, Yadav A, Shah SAA, Iqbal MAB, Ragab AE, Mahmoud HM. Qualitative analysis and soliton solutions of nonlinear extended quantum Zakharov-Kuznetsov equation. Nonlinear Dyn. 2024;112(21):19295-310.
22. Jiao L, Song X, You C, Liu X, Li L, Chen P, et al. AI meets physics: a comprehensive survey. Artif Intell Rev. 2024;57(9):256.
23. Youvan DC. Emergent thermodynamics: exploring complex mathematical dynamics in everyday systems. 2025.
24. Duan X, Peng G, Nazish HT, Li N, Ullah MS, Cheemaa N, Bekir A. Exploring soliton solutions and chaotic patterns in the Klein-Gordon equation for nuclear fission, fusion and plasma oscillations. Int J Theor Phys. 2025;64(11):320.
25. Ansari AR, Jhangeer A, Imran M, Alsubaie ASA, Inc M. Multi-dimensional phase portraits of stochastic fractional derivatives for nonlinear dynamical systems with solitary wave formation. Opt Quant Electron. 2024;56(5):823.

Received*: 10-10-2025 -* ***Accepted****: 08-12-2025 -* ***Published****: 16-12-2025*